
Article:
Kumararaja, P., Manjaiah, K.M., Datta, S.C. et al. (2 more authors) (2018) Chitosan-g-poly(acrylic acid)-bentonite composite: a potential immobilizing agent of heavy metals in soil. Cellulose, 25 (7). pp. 3985-3999. ISSN 0969-0239

https://doi.org/10.1007/s10570-018-1828-x

ABSTRACT

Aiming to achieve heavy metal adsorption in water and soil environments, a montmorillonite rich bentonite was graft-copolymerized with chitosan, and the obtained composite material was evaluated as a metal immobilizing agent for remediating metal contaminated soil. The graft-copolymerization reaction in the composite was confirmed by scanning electron microscopy (SEM), X-ray diffraction (XRD) and Fourier transform infrared spectroscopy (FTIR) techniques. Batch adsorption studies with varying experimental conditions, such as adsorbent amount, pH and metal concentration, were conducted to assess the metal adsorption capacity of the composite. The adsorption pattern followed the Langmuir isotherm model, and maximum monolayer capacity was 88.5, 72.9, 51.5 and 48.5 mg g^{-1} for Cu, Zn, Cd and Ni, respectively. Amendment of a contaminated soil with the composite enhanced the metal retention capacity by 3.4, 3.2, 4.9 and 5.6-fold for Cu, Zn, Cd and Ni, respectively, over unamended soil. The desorption percentage of metals from the composite treated soil was significantly lower than the unamended contaminated soil. The findings indicated that immobilization of heavy metals in soils could be achieved by the chitosan-bentonite, which would potentially be an inexpensive and sustainable environmental remediation technology.

Key words: Chitosan, Bentonite, Characterization, Adsorption, Metal contaminated soil, Remediation

1. Introduction

Heavy metal pollution by the discharge of metal laden effluents into the environment is one of the most serious environmental problems of modern society due to the toxic effects of metals on the ecosystem, agriculture, and human health. Removal of heavy metals from effluents before their disposal into the environment is essential since the metals are non-

biodegradable, may undergo chemical transformations and bio-magnification at different trophic levels.

Efficient, rational and economically feasible treatment technologies should be developed to overcome the issue of heavy metal pollution in the environment. Among the physico-chemical methods of heavy metal remediation, adsorption is easy to operate, and can treat waste effluents with high as well as very low metal loadings (Bolan et al. 2014; Gupta and Bhattacharya 2016). Biopolymers such as chitosan, cellulose and starch have been tested for removal of metals from effluents with varying degree of success. Chitosan with chelating hydroxyl (-OH) and amino (-NH) functional groups has been studied extensively for the treatment of metal laden wastewaters, but the material has poor mechanical stability (Azarova et al. 2016; Zhang et al. 2016). To overcome the weak mechanical stability, chitosan has been immobilized on an array of supporting materials (e.g., bentonite, zeolite) (Abdel Khalek et al. 2012; Liu et al. 2015; Ngah et al. 2013). In this regard, clay minerals with metal binding sites, mechanical stability, larger surface area and low cost could be used as potential support materials for improving chitosan stability and simultaneously enhancing metal removal performance of the composite materials **(**El-Dib et al. 2016; Grisdanurak et al. 2012; Futalan et al. 2011; Pestov and Bratskaya, 2016; Rusmin et al., 2015).

In the recent past, significant efforts have also been extended for the remediation of metal contaminated soils. Bringing down the risk level of contaminated soils to an acceptable limit (risk-based land management practices) can be a more rational method of soil remediation than expensive ex-situ and in-situ treatments (Naidu, 2013; Kumararaja et al., 2017). Stabilization of heavy metals in soils by immobilizing agents can reduce the availability of metals and their risk to a desired level (Lim et al., 2016; Sarkar et al., 2012). Due to their low costs, waste materials have been evaluated as soil metal stabilizers in numerous studies. However, many of these materials hold low metal

adsorption/immobilization capacities. Soil amendments with chelating functional groups, such as those delivered through natural polymers, are efficient for metal immobilization because of their ability to bind or complex the metal ions tightly (Etemadi et al. 2003; Kamari et al. 2011a; 2011b; Zhang et al. 2016; Shaheen et al. 2015a; Shaheen and Rinklebe, 2015; Yin et al. 2015).

Chitosan is a biopolymer that is easily available at cheap price from seafood wastes. Similarly, clay minerals are also abundantly available in almost all the continents. The objective of this work is therefore to improve the metal binding capacity of bentonite clay by synthesizing a chitosan-bentonite composite material through graft copolymerization method, and to evaluate the potential of the synthesized material as a metal immobilizing agent in water and soil. The chitosan-bentonite composite was characterized by X-ray diffraction (XRD), Fourier transform infrared (FTIR) and scanning electron mesoscopic (SEM) techniques, and its metal (Zn, Cu, Cd and Ni) adsorption capacity was evaluated by batch studies. Adsorption-desorption studies were also done to evaluate the composite material as an amendment for the remediation of contaminated soils by metal immobilization.

2. Materials and methods

2.1 Materials

Chitosan of low molecular weight (50-190 KDa) was procured from Sigma Aldrich Ltd., Mumbai, India. Ammonium per sulphate, acrylic acid, acetic acid and methylenebisacrylamide were purchased from Sisco Research Laboratories Pvt Ltd, India, and used without any purification. Bentonite was purchased from Minerals Ltd., New Delhi, India. Na-bentonite was prepared by adding NaCl solution (0.25 M) drop-wise to a 10% (w/v) bentonite suspension in deionized water (Kumararaja et al., 2017). Appropriate amount of analytical reagent (AR) grade salts of metals [$Ni(NO_3)_2.6H_2O$, $Cd(NO_3)_2.6H_2O$,

$Cu(SO_4)_2.5H_2O$, and $Zn(SO_4)_2.7H_2O$] were dissolved in deionized water to obtain stock solutions of metals (Zn, Cu, Ni and Cd) containing 1000 mg L^{-1} metal ions. The stock solution was diluted serially in deionized water to get the working standard solutions of metals. To evaluate the efficiency of chitosan-bentonite composite as an amendment for immobilizing metals, batch study was conducted using a metal contaminated soil. The soil was collected from agricultural fields continuously irrigated for more than two decades with the canal water of Bandi River, Rajasthan, India. The water was loaded with heavy metals discharged through untreated textile, tanning and electroplating effluents from the industries harbored in Pali industrial area, Rajasthan, India (Krishna and Govil, 2004; Dutta and Singh, 2014). The physico-chemical properties of the contaminated soil were determined by standard methods (Table 1).

Table 1. Physico-chemical properties of the industrial effluent irrigated heavy metal contaminated soil

Soil property	Value
Mechanical composition	
Sand (%)	57.00
Silt (%)	22.10
Clay (%)	20.90
Soil Texture	Sandy clay loam
pH (1:2)	8.65
EC (1:2) (dS m^{-1})	0.79
CEC (cmol (p^+) kg^{-1}	10.20
Soil organic carbon (%)	0.44
Available soil N (mg kg^{-1})	102.00
Available soil P (mg kg^{-1})	4.20
Available soil K (mg kg^{-1})	142.00
DTPA Extractable metal	
Zn (mg kg^{-1})	18.20
Cu (mg kg^{-1})	14.12
Ni (mg kg^{-1})	1.03
Total metal content	
Zn (mg kg^{-1})	158.70
Cu (mg kg^{-1})	48.40
Ni (mg kg^{-1})	33.60

2.2 Preparation of chitosan-g-poly(acrylic acid)-bentonite composite

Chitosan-g-poly(acrylic acid)-bentonite composite was prepared using graft co-polymerization method with minor modification of what was described previously (Zhang et al., 2007). Chitosan solution was prepared by dissolving 5 g of chitosan in 300 mL of 1% acetic acid with continuous stirring. The slurry was kept at 90°C for 5 h. After cooling to 60°C, N_2 was purged for 30 min. Aqueous solution of ammonium persulfate (APS) was added (0.94 g in 10 mL distilled water), and the reaction temperature was maintained at 60°C for 15 min. After cooling to 50°C, mixtures of 360 mL of acrylic acid, 1.198 g of N,N'-methylenebisacrylamide (MBA) and 4.79 g of Na-bentonite was added. The temperature was maintained at 70°C for 3 h under continuous stirring for the completion of grafting and polymerization reactions. Then the mixture was neutralized by the dropwise addition of 2 M sodium hydroxide. The completion of neutralization reaction was indicated by the appearance of a brown color. The whole procedure was done in a four-way neck reaction kettle. The final granular product was washed with distilled water, dried at 70°C, ground, sieved and desiccated to obtain the final chitosan-bentonite composite powder.

2.3 Characterization of chitosan-g-poly(acrylic acid)-bentonite composite

2.3.1 Cation retention capacity

Cation retention capacity of the composite was determined by Ca-Mg exchange method. The composite (200 mg) saturated with 0.25 M $CaCl_2$ was washed with 0.25 M $MgCl_2$ thrice to release the adsorbed Ca^{2+}. The supernatant was collected, and the volume was made up to 100 mL by distilled water. The Ca^{2+} concentration in the supernatant was determined by flame atomic absorption spectroscopy (ZEEnit 700, Analytic, Jena, Germany).

2.3.2 X-ray diffraction (XRD) analysis

XRD of the composite was performed at room temperature using Philips model PW1710 diffractometer to determine the changes in crystallinity of minerals. The diffractometer was fitted with a Cu tube (λ=1.5418 Å), and operated at 40 kV and 20 mA. The diffractograms were collected from 3° to 35° 2θ at a step size of 0.1° and counting rate of 5s per step using APD (automated powder diffraction) software.

2.3.3 FTIR spectroscopy

FTIR analyses were performed at room temperature by KBr disc method using a FTIR spectrophotometer; model SPECTRUM 1000, Perkin Elmer. KBr discs were prepared by mixing the chitosan-bentonite composite with IR grade KBr in pestle and mortar in the ratio of 1 mg composite per 100 mg of KBr. The mixture was pulverized to powder, and made into disc by a hydraulic press. The FTIR spectrum was recorded in the spectral range of 4000 – 600 cm^{-1} with a resolution of 4 cm^{-1} over 60 cumulative scans.

2.3.4 Scanning electron microscopy

To examine changes in the surface morphology of the composite, scanning electron microscopy (SEM) was used (EVO/MA10, CARL ZEISS Instruments). Prior to analysis the composite was coated with palladium in vacuum (10^{-3} Torr)

2.4 Batch adsorption and desorption experiments in water and soil

The metal adsorption capacity of the composite was examined using batch equilibrium experiments conducted at room temperature. The initial and equilibrium concentrations of metals in the aqueous solutions were analyzed by atomic adsorption

spectroscopy (AAS) as described earlier. Standard metal solutions procured from Merck (Darmstadt, Germany) was used to calibrate the spectrometer.

2.4.1 Effect of adsorbent dose

The dose of the composite was optimized by adding different masses of the material (0.01, 0.025, 0.05, 0.1, and 0.2 g) to 50 mL of 25 mg L^{-1} metal solution in polypropylene bottle. The mixture was equilibrated for 24 h based on a preliminary experiment in an agitating shaker. The metal solution pH was adjusted to pH=6 for Cu and Cd, pH=7 for Zn, and pH=8 for Ni with 0.01 M HCl or NaOH. The supernatant was obtained by filtration using Whatman No.42 filter paper at the end of the equilibration time.

2.4.2 Effect of pH

The effect of pH on metal adsorption was studied by shaking 0.1 g composite with 50 mL of 25 mg L^{-1} metal solutions adjusted at different pH values (1, 2, 3, 4, 5, 6, 7 and 8) for 24 h in polypropylene bottles.

2.4.3 Adsorption isotherm

Adsorption isotherms were obtained by shaking 50 mL of metal solutions of varying initial concentrations (0 to 100 mg L^{-1}) with 0.1 g of composite for 24 h on an end-to-end shaker at room temperature. Clear filtrate was obtained after the equilibration time by filtering through Whatman No.42 filter paper. Similar procedure was followed to obtain the metal adsorption capacity of unamended (1g soil) and amended soils (1g soil + 0.1g composite) with varying metal concentrations. A control (soil without added metal but only deionized water) was used, and the metal extracted in the control sample was deducted from

the others for calculating the final concentration to get adsorption isotherms (Forjan et al. 2016).

The metal adsorption capacity (q), the amount of ions adsorbed per unit mass of composite (mg g^{-1}) was determined by Eq. 1:

$$q_e = [(C_i - C_e)/m]\ V \qquad \text{(Eq. 1)}$$

where, q_e is the amount of metal ions adsorbed onto unit amount of the adsorbent (mg g^{-1}), C_i and C_e are the initial and equilibrium concentrations of metal in solution (mg L^{-1}), V is the volume of solution (L) and m is the mass of the adsorbent (g), respectively.

The metal removal efficiency, R, (%) of the chitosan-bentonite composite was calculated by Eq. 2:

$$R\ (\%) = [C_i - C_e / C_i] \times 100 \qquad \text{(Eq. 2)}$$

The distribution coefficient for adsorption was calculated using Eq. 3:

$$\text{Distribution coefficient } (K_d, \text{ mL } g^{-1}) := [C_i - C_e / C_i] * V / m \qquad \text{(Eq. 3)}$$

To study the effect of biopolymer-bentonite composite addition on heavy metal adsorption by soils, a procedure (Xiong et al. 2005; Tsadilas et al. 2009; Uchimiya et al. 2011; Li et al. 2016; Bogusz et al. 2017) similar to the aqueous system was followed. To 1 g soil, 0.05 g chitosan-bentonite composite was added, and the mixture was incubated for a fortnight at room temperature (25°C). Following incubation, 1g of amended soil was added to 30 mL of metal solutions (0.05 M $CaCl_2$ as the background electrolyte) with varying concentrations (5-50 mg L^{-1}), shaken for 24 h, and centrifuged at 8000 rpm for 15 min. After centrifugation, 15 mL of the supernatant was withdrawn and replaced with 15 mL of desorbing agents (0.05 M $Ca(NO_3)_2$, 0.05 M eethylenediaminetetraacetic acid or 0.05 M diethylenetriaminepentaacetic acid) to elucidate the desorption pattern. A similar procedure was followed for an unamended soil without addition of the composite.

2.5 Statistical analysis

The isotherm data of metal adsorption were fitted to the Langmuir and Freundlich models by nonlinear regression using least square method. The correlation coefficients (R^2) obtained from the regression analyses were used to evaluate the applicability of the isotherm equations.

3. Results and discussion

3.1 Characterization of chitosan grafted acrylic acid bentonite composite (chit-AA-bent)

Cation retention capacity is an important property of an adsorbent which determines its contaminant adsorption capacity. The cation retention capacity of chit-AA-bent composite was 95.5 cmol (p^+) kg^{-1} higher than that of bentonite (83.3 cmol (p^+) kg^{-1}). The XRD pattern (Fig. 1a) of bentonite showed a strong reflection at $2\theta = 6.8°$ which corresponded to a basal spacing of 12.2Å. This characteristic reflection corresponded to montmorillonite which is the predominant clay mineral (85%) in the bentonite clay. The XRD pattern shows the dominance of montmorillonite ($2\theta = 10.4°$, 12.6°, 19.4°) and impurities such as Quartz ($2\theta = 26.3°$, 29.4°) (JCPDS card No 13-0135). The intensity of the primary reflection of montmorillonite was reduced significantly following preparation of the chit-AA-bent composite (Fig. 1b). The shape of the typical montmorillonite reflection got flattened in case of the composite as against a sharp reflection in pristine bentonite, and the peak position was slightly shifted to the left ($2\theta = 5.9°$ and d = 14.9 Å) in the composite compared to the bentonite ($2\theta = 6.8°$) (Fig. 1b). The XRD patterns thus indicated that intercalation of the polymer into the stacked silicate galleries of bentonite (montmorillonite) led to an exfoliation of the clay mineral in the polymer matrix to form a composite structure (Sarkar 2009; El-Sherif and El-Masry 2011; Liu et al. 2015). Many studies indicate the disappearance of

characteristic montmorillonite peak and appearance of other peaks in the composites (Yadav and Rhee, 2012; Ma et al., 2012)

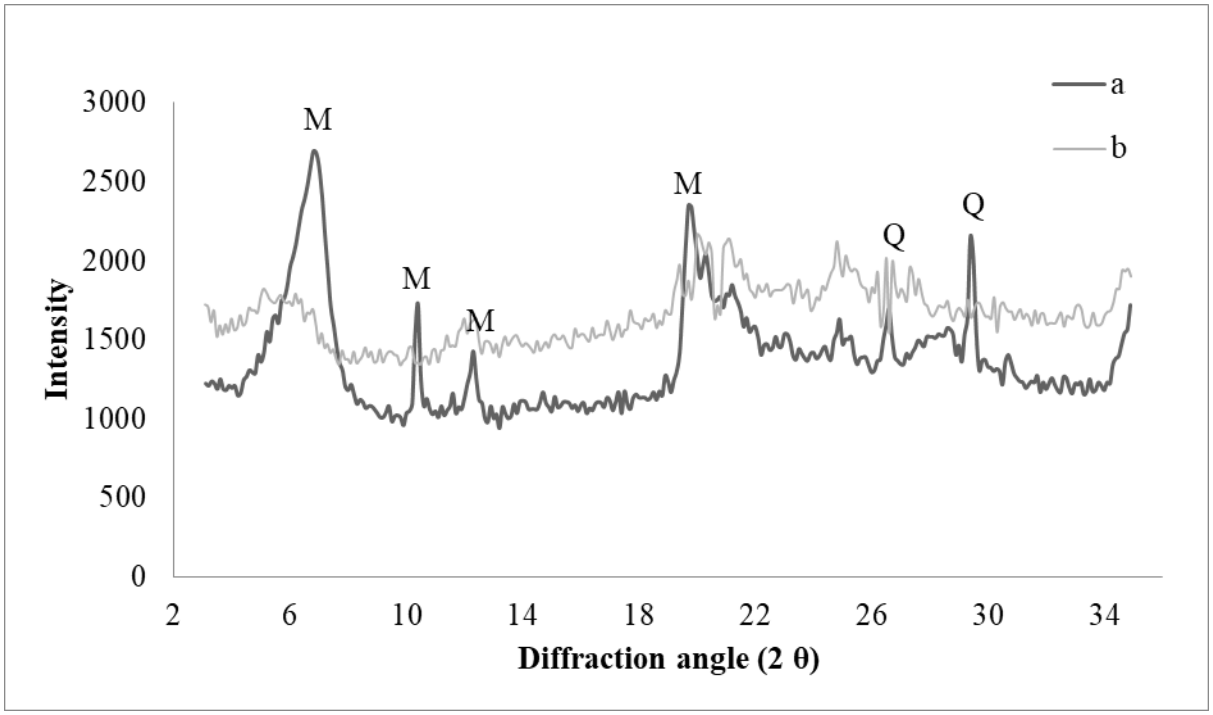

M-Montmorillonite, Q-Quartz

Fig. 1. Randomly oriented XRD pattern of (a) bentonite, and (b) chitosan grafted bentonite composite

To obtain further evidence on clay exfoliation and composite formation, FTIR spectra of raw bentonite, chitosan and chit-AA-bent composite were recorded in the region of 4000 – 600 cm^{-1} (Fig. 2). Disappearance of characteristic absorption bands of amide I (1653cm^{-1}) and N-H (1596 cm^{-1}) in the spectrum of the composite confirmed that these reactive functional groups (-NH_2 and –NHCO) in chitosan took part in the graft reaction with acrylic acid (Sarkar 2009; Xie and Wang, 2009; Abdel Kalek et al., 2012). The absorption bands at 1558 and 1414 cm^{-1} in the spectrum of the composite were arisen from acrylic acid, and could be assigned to asymmetric and symmetric –COO− stretching vibrations, respectively

(Bulut and Karaer, 2014; Raifei et al., 2016). The characteristic bands in the spectrum of Na-bentonite at 3697 and 1637 cm^{-1} (stretching and bending vibrations of -OH) also disappeared in the spectrum of the composite. The polymerization reaction between chitosan, AA and bentonite in the composite was confirmed by the disappearance of Si-O stretching vibration at 1032 cm^{-1}, and appearance of a new band at 1022 cm^{-1}. Overall, FTIR spectra of the materials indicated that Na-bentonite participated in the grafting copolymerization reaction through its active Si-OH groups (Paluszkiewicz et al. 2011; Luo et al. 2015).

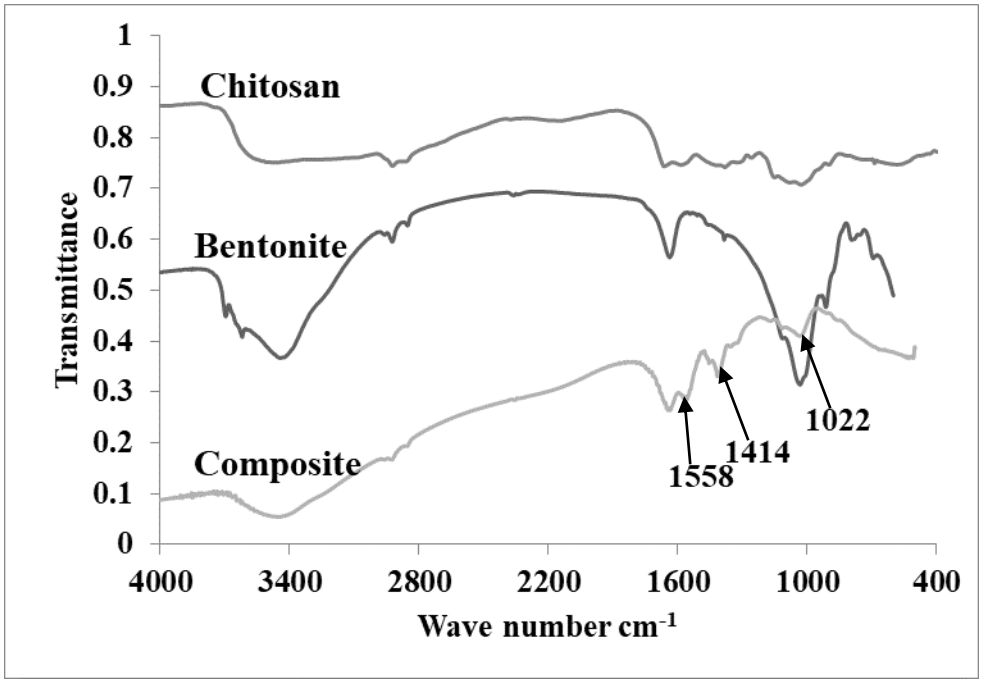

Fig. 2 FTIR spectra of chitosan, bentonite, and chitosan grafted bentonite composite

The scanning electron micrograph of the composite (Fig. 3) revealed a more extensive unfolded 3D network of the material, which could be attributed to the cross-linking reaction leading to the formation of closely packed chain rearrangement of polymer and clay particles (Abdel Kalek et al., 2012; Hafida et al., 2014). The SEM image of the composite verified that the material contained a porous structure (Lewandowska et al. 2014; Costa et al. 2016).

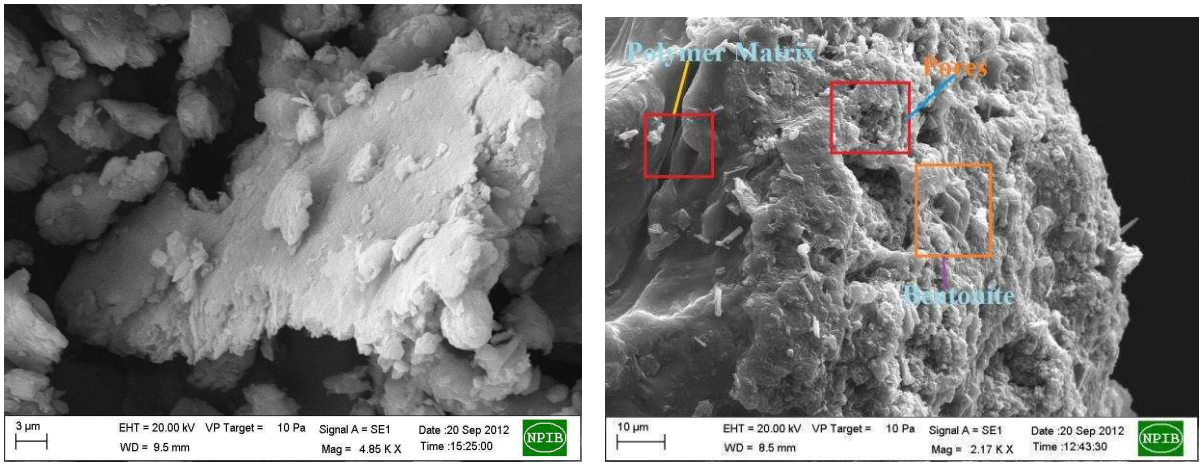

Figure 3. Scanning Electron Microscopy images of (a) bentonite, and (b) chitosan grafted bentonite composite

3.2 Adsorption of heavy metals

3.2.1 Effect of adsorbent dose

Results indicated that percentage removal of metals increased from 60% to 95%, 35% to 95%, 20% to 85% and 30% to 70% in case of Cu(II), Zn(II), Cd(II) and Ni(II), respectively, with the increasing adsorbent doses (Fig. 4a). An increase in the effective surface area and exchangeable sites for metal ions with increasing dose of the adsorbent resulted in higher percentage of metal removal. Contrarily, as the composite dose increased, the metal adsorption capacity decreased (Fig. 4b). In this case, the concentration of metal ions became a limiting factor to cover the available exchangeable sites leading to a large number of unoccupied sites. Reduced efficiency of metal adsorption by the composite at higher dose might also arise from the decreased total surface area and increased diffusional path due to aggregation of composite particles (Ngah et al. 2013; Wang et al. 2014; Tsai et al. 2016).

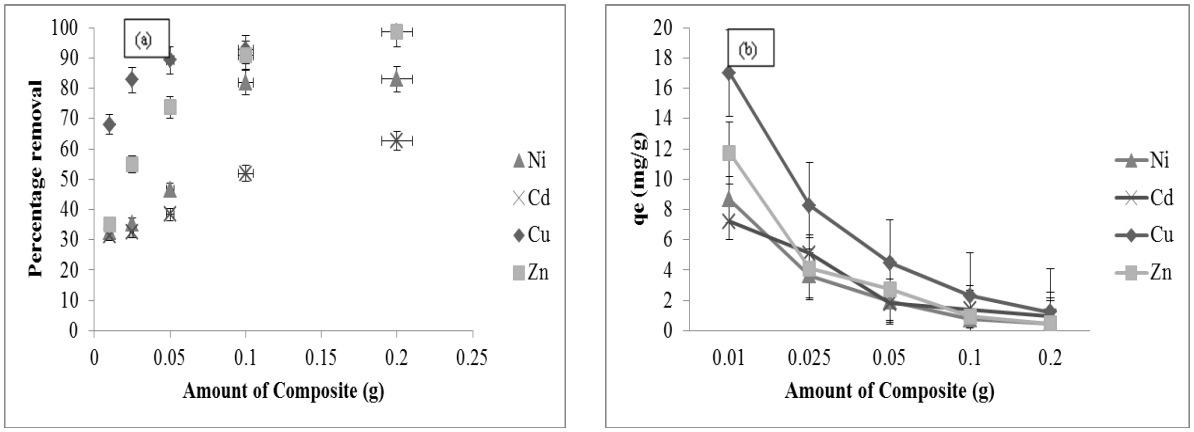

Figure 4. Effect of adsorbent dose on percentage removal (a) and sorption capacity (b) of Zn, Cu, Ni and Cd by chitosan grafted bentonite composite

3.2.2 Effect of pH

The speciation and distribution of metal ions, degree of ionization of the composite and the counter ion concentration can be influenced by the solution pH, and thereby it can control the adsorption process. Depending on the pH, the active sites (OH, COOH, NH_2) on chit-AA-bent composite could either be protonated or deprotonated. Adsorption of metals at equilibrium was low at acidic pH, and it increased with increasing pH of the solution up to a critical pH level (Fig. 5). Results indicated that Cu(II) and Cd(II) were adsorbed at maximum levels onto the composite at pH 6, whereas maximum Zn(II) and Ni(II) adsorption occurred at pH 7 and 8, respectively. Increased levels of H^+ and hydronium (H_3O^+) ions at lower pH values would decrease metal adsorption by the composite due to a competition among cations for the adsorption sites (Rusmin et al., 2016). The repulsive electrostatic force induced towards the approaching cations by the positively charged surface arisen from the protonated amino groups ($-NH_3^+$) of the composite at acidic pH would thus result in a reduced metal uptake (Grisdanurak et al. 2012; Zhang et al. 2016; Duan et al. 2016). The following reaction (Eq. 4) shows the influence of pH on metal adsorption by the chit-AA-bent composite:

$$\text{Composite–}NH_3^+ + M^{2+} \longrightarrow \text{Composite–}NH_2 - M^{2+} + H^+ \qquad \text{(Eq. 4)}$$

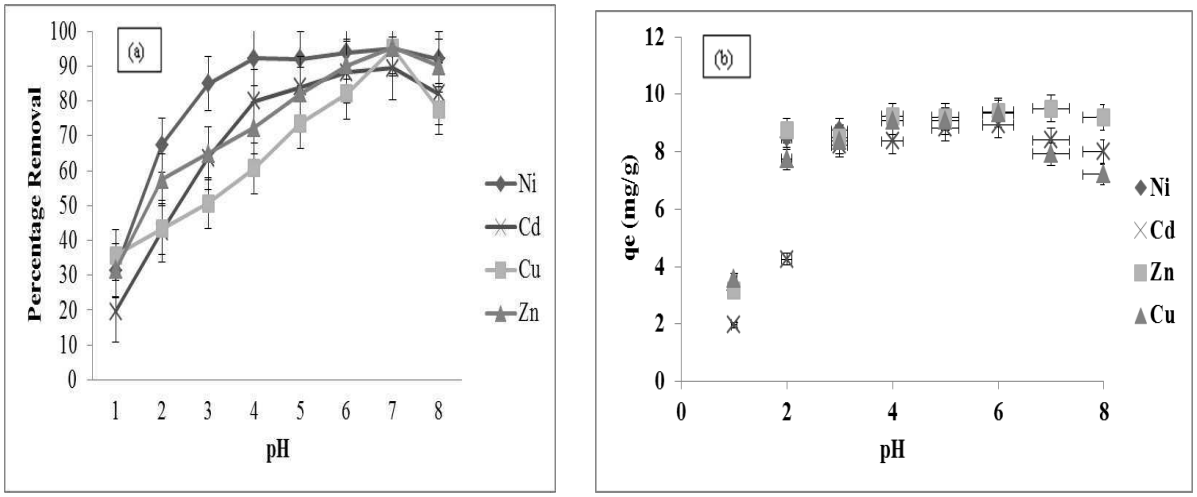

Figure 5. Effect of pH on percentage removal (a) and sorption capacity (b) of Zn, Cu, Ni and Cd by chitosan grafted bentonite composite

On the other hand, development of negative charges at higher pH by deprotonation of surface functional groups attracted the metal cations by electrostatic interaction. The smothering of the inhibitory effect of H^+ ions also resulted in enhanced metal adsorption. However, precipitation of metals as metal hydroxides above the critical pH value (> 6 for Cu and Cd) resulted in a decreased adsorption. The mechanism of metal adsorption by an adsorbent with functional groups at different pH can be represented by Eq. 5.

$$M^{2+} + RNH_2 \longrightarrow M(RNH_2)^{2+} \qquad \text{(Eq. 5)}$$

The amino group of the composite might react with hydrogen ions (H^+) as in Eq. 6:

$$H^+ + RNH_2 \longrightarrow H(RNH_2)^+ \qquad \text{(Eq. 6)}$$

$$OH^- + RNH_2 \longrightarrow (RNH) + H_2O \qquad \text{(Eq. 7)}$$

3.2.3 Adsorption isotherms

The Langmuir isotherm (Eq. 8) describes the adsorption onto a homogenous surface.

$$q_e = \frac{q_m K_L C_e}{1 + K_L C_e} \qquad \text{(Eq. 8)}$$

where, q_e is the equilibrium adsorption capacity (mg g^{-1}), C_e is the equilibrium concentration of metal (mg L^{-1}), q_m is the maximum amount of metal adsorbed per unit weight of the composite, K_L is the Langmuir constant (L mg^{-1}) is measure of energy of adsorption. q_m and K_L are obtained from the slope and intercept of linear plot of C_e/q_e against C_e. A dimensionless constant (known as separation factor or equilibrium factor; R_L) (Foo and Hameed, 2010; Wang et al., 2014) calculated from the Langmuir constants (Eq. 9) can be used to predict whether the adsorption process is unfavorable (R_L >1), linear (R_L = 1) favorable (0< R_L<1) or irreversible (R_L =0).

$$R_L = \frac{1}{1+K_L C_i} \qquad \text{(Eq. 9)}$$

The Freundlich isotherm is an empirical equation (Eq. 10) which describes the heterogeneous surface adsorption.

$$q_e = K_f \times C^{1/n} \qquad \text{(Eq. 10)}$$

where, q_e is the amount of metal ion adsorbed (mg g^{-1}) onto the composite. The Freundlich parameters K_f and n represent the adsorption capacity and intensity, respectively. Slope and intercept of the linear plots of log q_e versus log C_e (log q_e = log K_f + 1/n log C_e) gives K_f and n. The favorability of the adsorption process is indicated by the Freundlich constant n value; values < 1 for poor adsorption, 1-2 for moderately good, and 2-10 represent the beneficial adsorption (Foo and Hameed, 2010; Sarkar et al., 2012).

Langmuir isotherm model fitted well with the adsorption data for the studied metals with R^2 values ≥ 0.98 (Table 2). This suggested the occurrence of monolayer adsorption on an energetically uniform surface (Pereira et al. 2013; Moussout et al. 2016). The Langmuir maximum monolayer adsorption capacity (q_m) of the composite were in the following order: Cu: 88.49, Zn: 72.99, Cd: 51.55 and Ni: 48.54 mg g^{-1}. The adsorption capacity of the composite was higher than that of the raw bentonite (Cu:13.95, Zn:11.41, Cd:9.41, Ni:13.95

mg g^{-1}) (Kumararaja et al., 2014; Kumararaja and Manjaiah, 2015). The sequence of metal adsorption by the composite is in agreement with previous results (Ngah et al. 2011; Kamari et al., 2012a&b). The intrinsic nature of metal ions has an important influence on their adsorption performance. High electronegativity, high softness value and easy hydrolyzability would result in preferential adsorption of Cu (II) over other ions. The metal adsorption sequence followed negative log of the first hydrolysis dissociation constant of the metals [Cu (8.0); Zn (9.0); Ni (9.9) and Cd (10.1)]. Metals with low hydrolysis constant easily form hydroxo-complex which is adsorbed to the composite more strongly than the free ions. Similar to hydrolysis constant, the adsorption of metals also followed the electronegativity parameters [Cu (2.0); Ni (1.91); Cd (1.69) and Zn (1.65)] of metals except for Zn. Electronegativity of a metal ion is the ability to attract electrons towards itself to form a bond with another atom or ion. As the difference in electronegativity is large for Cu, it is preferentially adsorbed onto the composite. Metals with large softness value has a higher affinity for forming electrostatic and inner sphere complexes with an adsorbent. The higher the covalent index of metal ions, higher is the affinity for the adsorption site. Metals having high hardness index (5.55, 5.40 and 4.12 for Cu, Zn and Cd, respectively) are easily polarizable, and have high affinity for ligand molecules. The dominance of Cu in the affinity sequence reinforced the role of specific binding mechanisms such as covalent binding to composite surfaces with high stability and binding energy in the behaviour of this metal. Ni, Zn and Cd are more affected by the electrostatic interactions with the surface exchange sites. The K_L related to the affinity of binding sites showed the highest value for Cu (Usman 2008; Jalali and Moradi 2013; Tsai et al., 2016). Chit-AA-Bent metal sorption capacity is compared with previously reported chitosan-based adsorbents (Supplementary)

Table 2. Isotherm constants and correlation coefficients for metal sorption on chitosan biopolymer bentonite composite in aqueous system

Parameters	Zn	Cu	Ni	Cd
Langmuir adsorption isotherm				
q_m (mg g^{-1})	72.99	88.49	48.54	51.55
K_L (L mg^{-1})	0.66	0.45	0.18	0.17
R^2	0.99	0.98	0.99	0.98
Freundlich adsorption isotherm				
K_f (mg g^{-1}) (L g^{-1})$^{1/n}$	21.86	30.62	10.66	10.77
N	2.92	6.21	2.42	2.62
R^2	0.77	0.93	0.98	0.97

The R_L values (Table 3) varied between 0.60 to 0.04 for Zn, 0.69 to 0.05 for Cu, 0.88 to 0.13 for Cd and 0.85 to 0.12 for Ni. The R_L values at metal concentrations of 5-50 mg L^{-1} were in the range of $0< R_L < 1$, which indicated that the adsorption of Zn, Cu, Ni and Cd ions onto the composite was favorable. It implied that the composite was an efficient adsorbent for the removal of Cu(II), Zn(II), Cd(II) and Ni(II) (Futalan et al. 2011; Saravanan et al. 2011; Azzam et al., 2016).

Table 3. Langmuir isotherm dimensionless separation factor (R_L) values

Initial metal concentration (mg L^{-1})	R_L values			
	Zn	Cu	Ni	Cd
5	0.60	0.69	0.85	0.85
10	0.23	0.31	0.53	0.54
20	0.13	0.18	0.34	0.37
30	0.07	0.10	0.22	0.23
40	0.05	0.07	0.16	0.16
50	0.04	0.05	0.12	0.13

The Freundlich parameters along with the correlation coefficients are given in Table 2. Copper (II) had the highest K_f and n values over Zn(II), Cd(II) and Ni(II). Higher n value for Cu (II) indicated that the functional groups of the composite had greater affinity towards it, and the larger K_f values could be ascribed to the strong binding of Cu(II) by the composite. The n values for the studied metals lie between 1 and 10 indicating beneficial adsorption of metals by the chit-AA-bent composite. The order of n for the metals was Cu(II) > Zn(II) > Cd(II) > Ni(II) corresponding to the adsorbability or adsorption affinity sequence, which was also in agreement with the adsorption data. Isotherms with n > 1 are classified as L-type

isotherms reflecting high affinity between adsorbate and adsorbent, which is indicative of chemisorption (Duan et al., 2016). Higher n values indicated that the adsorption sites were more of heterogeneous in nature (Liu et al. 2015; El-Dib et al. 2016; Moussout et al. 2016).

3.2.4 Distribution coefficients

The K_d values over the studied initial metal concentrations are shown in Fig. 6. The K_d values indicate a preference of the adsorbent towards the adsorbate (metal ions), the higher is the K_d value, greater is the adsorbent-adsorbate affinity. The K_d values were found to be the highest for Cu(II) followed by Zn(II), Cd(II), and the least for Ni(II). Cu and Zn were adsorbed strongly, whereas Cd and Ni showed a weaker affinity. As the nature of adsorption sites changes with the metal concentrations, the K_d values also decrease at higher metal concentrations. Sites with strong binding energies exhibit high selectivity towards the metals at a lower concentration. As the metal concentration increases, the K_d values decreases due to specific sites are continuously occupied by the metals resulting in non-specific adsorption (Gomes et al. 2001; Shaheen et al. 2013; Sastre et al. 2006; Souza Baraz et al. 2013).

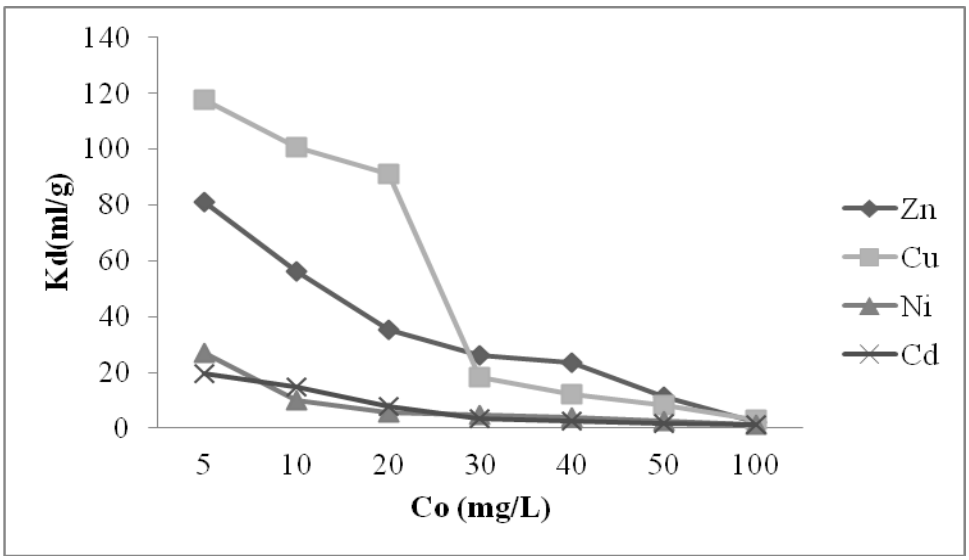

Figure 6. Distribution coefficients of metals with varying initial metal concentrations

3.2.5 Desorption of metals

Desorption study was conducted with three different desorbing agents, namely calcium nitrate [$Ca(NO_3)_2$], EDTA and DTPA at 0.05 M concentrations. Among the desorbing agents, the electrolyte, $Ca(NO_3)_2$, was found to be ineffective in removing the adsorbed metals from the composite (Fig. 7). Contrarily, owing to their metal chelating functional groups, the organic desorbing agents were able to remove up to 90% of the adsorbed metals. Hence, either EDTA or DTPA could be utilized for regenerating the composite when applied for water purification (Ngah et al. 2013; Pereira et al. 2013; Davari et al. 2015; Luo et al. 2015). On the other hand, a lower desorption of adsorbed metals from the composite in the presence of $Ca(NO_3)_2$ makes the material suitable for immobilizing metals in contaminated soils where an environmental electrolyte concentration always exists.

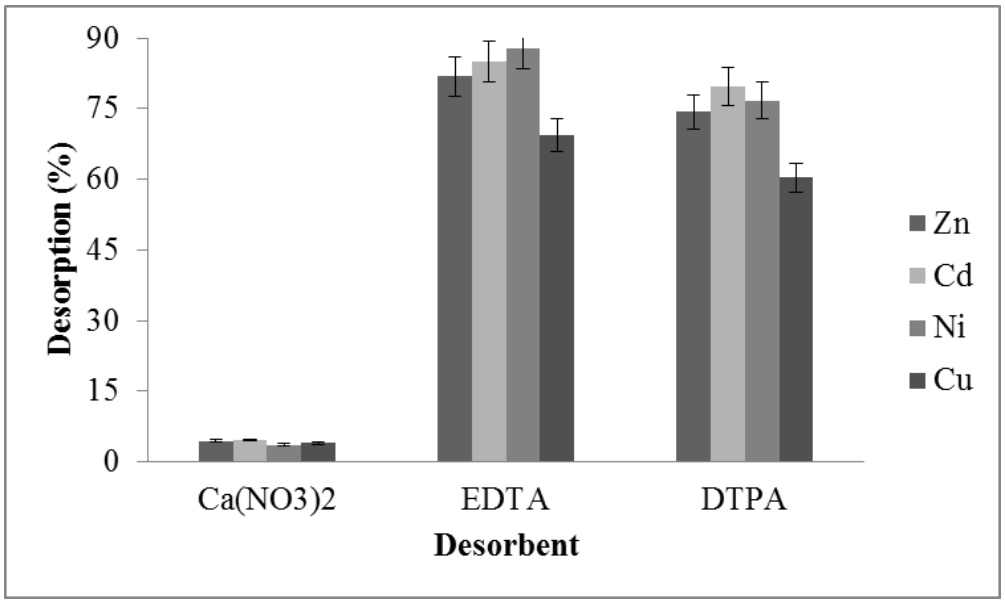

Figure 7. Desorption percentage of metals from chitosan grafted bentonite composite by different desorbing agents

3.2.6 Metal immobilization in soils

The contaminated soil used for the adsorption study was alkaline in reaction (pH in

1:2 soil: water =8.65), sandy clay loam in texture, with oxidizable organic carbon content of 4.43 mg kg^{-1} (Table 1). The Langmuir parameters and correlation coefficients of metal adsorption (Zn, Cu, Ni and Cd) by contaminated soil in the absence and presence of chit-AA-bent are shown in Table 4. The Langmuir model described the adsorption data better than Freundlich model for all the metals in case of the unamended contaminated soil. Langmuir maximum monolayer adsorption capacity of the contaminated soil (unamended) was 0.85, 0.94, 0.45 and 0.42 mg g^{-1} for Zn(II), Cu(II), Cd(II) and Ni(II), respectively, and the affinity of metals was in the order Cu(II) > Zn(II) > Ni(II) > Cd(II). Application of the chit-AA-bent composite increased the monolayer maximum adsorption capacity of the contaminated soil by 3.4, 3.2, 4.9 and 5.6 times for Zn, Cu, Ni and Cd, respectively. The maximum adsorption capacity of contaminated soil for the studied metals increased in the presence of the composite due to the increased adsorption sites available for the metals on the composite surfaces. The relative increase of Cd and Ni adsorption was higher than that of Cu. The effect of the chit-AA-bent composite treatment increased the adsorption capacity of weakly adsorbing heavy metals such as Ni, Cd and Zn compared to the strongly adsorbing metal such as Cu. This might be due to the inherent high adsorption capacity of the contaminated soil for Cu because of the higher organic matter content with the different chelating functional groups (Ye et al., 2013; Rinklebe and Shaheen 2015). The large difference in q_m value between water and soil is due to the lower metal adsorption capacity of soil (0.85, 0.94, 0.45 and 0.42 mg g^{-1}) for Zn(II), Cu(II), Cd(II) and Ni(II), respectively). In soil, only 10% of sites (composite) are with higher metal adsorption capacity and remaining 90% are with lower adsorption capacity. Similarly, Fernández-Pazos et al (2016) reported that the Cr adsorption capacity of mussel shell was 121,878 mg kg^{-1}, but the same in soil amended with mussel shell was only 677 mg kg^{-1}. The Langmuir parameter K_L represents the binding energy coefficient which corresponds to adsorbate concentration at which the amount of metal bound to the

adsorbent is equal to $q_m/2$ (Sastre et al. 2006). The K_L values for the contaminated soil were 1.09, 0.24, 0.16 and 0.10 for Cu, Zn, Ni and Cd, respectively, indicating a significantly stronger affinity of the soil for Cu than other metals. The Freundlich model described the adsorption data better for the contaminated soils that were amended with the chit-AA-bent composite (Table 4). The K_f and N values were 15.53, 15.11, 12.16, 10.81, and 3.09, 2.17, 2.04, 1.59, respectively, for Cu, Zn, Cd and Ni. The N values for all the metals studied was greater than 1, reflecting a favorable adsorption (Kamari et al. 2011a; 2011b; Ming et al. 2016).

Table 4. Isotherm constants and correlation coefficients for metal sorption on contaminated soil treated with chitosan biopolymer bentonite composite

Langmuir adsorption isotherm				
Soil				
	Zn	Cu	Ni	Cd
Qm (mg g^{-1})	0.85	0.94	0.42	0.45
K_L (L g^{-1})	0.24	1.09	0.10	0.16
R^2	0.99	0.99	0.99	0.99
Soil + Chit-AA-bent composite				
Qm (mg g^{-1})	2.91	3.06	2.09	2.53
K_L (L g^{-1})	0.07	0.10	0.02	0.06
R^2	0.97	0.91	0.95	0.95
Freundlich adsorption isotherm				
Soil				
K_f (mg g^{-1}) (L g^{-1})$^{1/n}$	5.05	8.41	1.58	4.71
N	1.42	1.53	1.27	1.41
R^2	0.95	0.97	0.91	0.90
Soil+ Chit-AA-bent composite				
K_f (mg g^{-1}) (L g^{-1})$^{1/n}$	15.11	15.53	10.81	12.16
N	2.17	3.09	1.59	2.04
R^2	0.99	0.99	0.99	0.99

The term ‘adsorption intensity’ is the ratio of the quantity adsorbed in the solid phase to the initial solution quantity of the adsorbate. The adsorption intensities of metals on the composite-amended or unamended soils (Table 5) showed a decreasing trend with the increasing initial metal concentrations. At a lower initial metal loading, there was insignificant difference in adsorption intensities between the amended and unamended soils.

It was because of the sufficient unoccupied adsorption sites available for metals. But at a higher initial metal loading, a higher concentration of metals remained in the solution in the unamended soils that resulted in a lower adsorption intensity. Composite addition to the soil increased the adsorption sites that resulted in more amount of metals in the solid phase leading to a higher adsorption intensity than that of the untreated soil. Among the metals studied, Cu maintained a higher adsorption intensity due to higher affinity for adsorption sites than that of Zn, Cd and Ni in the treated and untreated soils (Shaheen et al. 2013; Srinivasarao et al. 2014; Shaheen et al. 2015a &b; Kang et al. 2016).

Table 5. Sorption intensities of metals on contaminated soil with and without chit-AA-bent composite

C_i	Cu		Zn		Ni		Cd	
(mg L^{-1})	Soil + chit-AA-bent composite	Soil	Soil + chit-AA-bent composite	Soil	Soil + chit-AA-bent composite	Soil	Soil + chit-AA-bent composite	Soil
5	97.4	88.8	90.2	71.8	88.0	55.9	86.8	78.0
10	98.4	87.4	87.6	62.6	86.5	50.8	86.1	63.1
20	93.5	78.0	87.0	53.6	80.5	46.8	82.6	54.3
30	85.2	74.7	82.2	46.9	73.5	37.2	80.4	43.5
40	81.6	68.4	81.6	46.6	75.3	28.3	81.6	33.8
50	79.5	60.8	78.6	39.1	74.5	27.0	77.5	26.5

Desorption rate can be used to characterize the degree of metal binding to the adsorbent. Higher the percentage of desorption, the weak the binding. The desorption of all the metals were decreased in the presence of the chit-AA-bent composite from the contaminated soil compared to the unamended soil (Fig. 8). The desorption percentage was higher at a higher metal loading for all the studied metals both in the presence and absence of the composite. Desorption percentages at all initial metal concentrations were lower for the strongly adsorbed metal Cu (0.02% at 5 ppm to 0.27% at 50 ppm) than that of Zn (0.07% at 5 ppm to 3.03% at 50 ppm), Cd (0.2% at 5 ppm to 6.41% at 50 ppm), Ni (0.62% at 5 ppm to

5.58% at 50 ppm) in the amended soil. The percentage desorption sequence followed the same trend as in the unamended soil, and the percentage desorption was 4.26% at 5 ppm to 16.9% at 50 ppm, 6.66% at 5 ppm to 26.8% at 50 ppm, 10.5% at 5 ppm to 31.12% at 50 ppm and 10.6% at 5 ppm to 37.3% at 50 ppm for Cu, Zn, Cd and Ni, respectively. Lowered desorption of metals in the composite amended soil might be due to the strong binding of metals by the chelating functional groups of the composite. The lower percentage of desorption of Cu might be because of the formation of multinuclear complexes with the composite. Increased desorption at higher loading might be due to adsorption at edges of the composite (Futalan et al., 2012; Arabyarmohammadi et al., 2016). For the studied metals, the desorption sequence followed their relative stability of the ligand complexes.

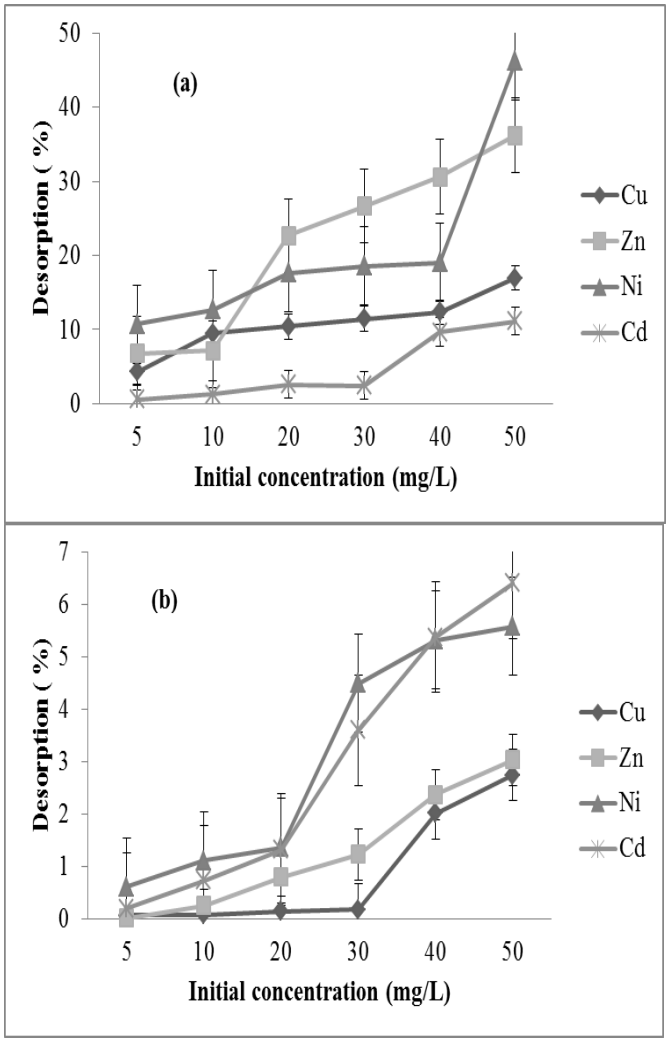

Figure 8. Desorption percentage of metals from (a) unamended contaminated soil and (b) chitosan grafted bentonite composite-amended contaminated soil

4. Conclusions

XRD and SEM analyses confirmed that the layers of montmorillonite in bentonite were mostly exfoliated and dispersed in the organic matrix to form a porous composite structure of chit-AA-bent. Similarly, the FTIR spectra confirmed the participation of montmorillonite particles in the grafting copolymerization reaction through its active Si-OH groups to form the biopolymer composite of desired properties. The Cu, Zn, Cd and Ni adsorption capacities of the chit-AA-bent composite were higher than that of the pristine bentonite. Amongst the adsorption isotherms, Langmuir equation fitted well, and the study demonstrated the usefulness of biopolymer composite in removing metals from aqueous solutions by adsorption mechanism, i.e., through chelating interaction between functional groups of composite and metals. The Freundlich adsorption model was fitted well to the adsorption data of the composite-amended metal contaminated soil. The biopolymer composite enhanced the adsorption intensity of metals in the contaminated soil and lowered desorption of metals. Thus, the composite material could be used as a potential immobilizing agent for remediating heavy metals in contaminated soils.

Acknowledgements

Authors thank the Head, Division of Soil Science and Agricultural Chemistry, ICAR-Indian Agricultural Research Institute, New Delhi, India for providing all the required facilities to carry out the present investigation.

5. References:

Abdel KMA, Mahmoud GA, El-Kelesh NA (2012) Synthesis and characterization of poly-methacrylic acid grafted chitosan-bentonite composite and its application for heavy metals recovery. Chem Mater Res 2: 1–12

Arabyarmohammadi H, Darban AK, Abdollahy M, Yong R, Ayati B, Zirakjou A, van der Zee SEATM (2017) Utilization of a novel chitosan/clay/biochar nanobiocomposite for immobilization of heavy metals in acid soil environment. J Polym Environ 1-13.

Azarova YA, Pestov AV, Bratskaya SY (2016) Application of chitosan and its derivatives for solid-phase extraction of metal and metalloid ions: a mini-review. Cellulose 23(4): 2273-2289

Azzam EMS, Eshaq G, Rabie AM, Bakr AA, Abd-Elaal AA, El Metwally AE, Tawfik SM (2016) Preparation and characterization of chitosan-clay nanocomposites for the removal of Cu(II) from aqueous solution. Int J Bio Macromolecules 89: 507–517

Bogusz A, Oleszczuk P, Dobrowolski R (2017) Adsorption and desorption of heavy metals by the sewage sludge and biochar-amended soil. Environ Geochem Health http://dx.doi.org/10.1007/s10653-017-0036-1

Bolan N, Kunhikrishna A, Thangarajan R, Kumpiene J, Park J, Makino T, Kirkham MB, Scheckel K (2014) Remediation of heavy metal(loid)s contaminated soils- to mobilize or to immobilize? J Hazard Mater 266: 141–166

Bulut B, Karaer K (2014) Removal of methylene blue from aqueous solution by crosslinked chitosan-g-poly (acrylic acid) / bentonite composite. Chem Eng Commun 202(12):1635-1644

Carter DL, Heilman MC, Gonza´lez CL (1965) Ethylene glycol monoethyl ether for determining surface area of silicate minerals. Soil Sci 100:356–360

Costa MPM, Ferreira ILM, Cruz MTM (2016) New polyelectrolyte complex from pectin/chitosan and montmorillonite clay. Carbohydr Polym 146: 123–130

Davari M, Rahnemaie R, Mehdi (2015) Competitive adsorption-desorption reactions of two hazardous heavy metals in contaminated soils. Environ Sci Pollut Res 22:13024–13032

Dias MV, Azevedo VM, Borges SV, Soares NFF, Fernandes RVB, Marques JJ, Medeiros EAA (2014) Development of chitosan / montmorillonite nanocomposites with encapsulated a-tocopherol. Food Chem 165: 323–329

Duan L, Hu N, Wang T, Wang H, Ling L, Sun Y, Xie X (2016) Removal of copper and lead from aqueous solution by adsorption onto cross-linked chitosan/montmorillonite nanocomposites in the presence of hydroxyl–aluminum oligomeric cations: equilibrium, kinetic, and thermodynamic studies. Chem Eng Comm 203(1): 28-36

Dutta S, Singh S (2014) Assessment of ground water and surface water quality around industrial area affected by textile dyeing and printing effluents, Pali, Rajasthan, India. J Environ Res Devel 8: 574 -581

El-Dib FI, Hussein MH, Hefni HH, Eshaq G, ElMetwally AE (2014) Synthesis and characterization of crosslinked chitosan immobilized on bentonite and its grafted products with polyaniline. J Appl Polym Sci 131: 41078–41084

El-Dib FI, Tawfik FM, Hefni HHH, Eshaq GH, ElMetwally AE (2016) Remediation of distilleries wastewater using chitosan immobilized bentonite and bentonite based organoclays. Int J Biol Macromolecules 86:750-755

El-Sherif H, El-Masry M (2011) Superabsorbent nanocomposite hydrogels based on intercalation of chitosan into activated bentonite. Polym Bull 66:721-734

Etemadi O, Petrisor IG, Kim D, Wan M-W, Yen TF (2003) Stabilization of metals in subsurface by biopolymers: laboratory drainage flow studies. Soil Sediment Contam 12:647–661

Fernández-Pazos MT, Garrido-Rodriguez B, Nóvoa-Muñoz JC, Arias-Estévez M, Fernández-Sanjurjo M J, Núñez-Delgado A, E. Álvarez E (2013) Cr(VI) Adsorption and desorption on soils and biosorbents. Water Air Soil Pollut 224:1366-1378

Foo KY, Hameed BH (2010) Insights into the modeling of adsorption isotherm systems. Chem Eng J 156:2–10

Forján R, Asensio V, Rodríguez-Vila A, Covelo EF (2016) Contribution of waste and biochar amendment to the sorption of metals in a copper mine tailing. Catena 137: 120–125

Futalan CM, Kan CC, Dalida ML, Hsien KJ, Pascua C, Wan MW (2011) Comparative and competitive adsorption of copper, lead, and nickel using chitosan immobilized on bentonite. Carbohyd Polym 83: 528-536

Futalan CM, Tsai WC, Lin SS, Hsien KJ, Dalida ML, Wan MW (2012) Copper, nickel and lead adsorption from aqueous solution using chitosan-immobilized on bentonite in a ternary system. Sustain. Environ Res. 22(6): 345-355

Gomes PC, Fontes MPF, da Silva AG, Mendonca ED, Netto AR (2001) Selectivity sequence and competitive adsorption of heavy metals by Brazilian soils. Soil Sci Soc Am J 65:1115–1121

Grisdanurak N, Akewaranugulsiri S, Futalan CM, Tsai WC, Kan CC, Hsu CW, Wan MW (2012) The study of copper adsorption from aqueous solution using crosslinked chitosan immobilized on bentonite. J Appl Polym Sci 125: 132–142

Gupta SS, Bhattacharya KG (2016) Adsorption of metal ions by clays and inorganic solids. RSC Adv 4: 28537-28586

Hafida FH, Aiouaz N, Dairi N, Hadj-Hamou AS (2014) Preparation of chitosan-g-poly(acrylamide)/montmorillonite superabsorbent polymer composites: studies on swelling, thermal, and antibacterial properties. J Appl Polym Sci 131: 39747

Houben D, Pircar J, Sonnet P (2012) Heavy metal immobilization by cost-effective amendments in a contaminated soil: Effects on metal leaching and phytoavailability. J Geoche Explor 123: 87–94

Jalali M, Moradi F (2013) Competitive sorption of Cd, Cu, Mn, Ni, Pb and Zn in polluted and unpolluted calcareous soils. Environ Monit Assess 185(11):8831-46

Jiang W, Tao T, Liao Z (2011) Removal of heavy metal from contaminated soil with chelating agents. Open J Soil Sci 1: 70-76

Kamari A, Pulford ID, Hargreaves JSJ (2011a) Binding of heavy metal contaminants onto chitosans—an evaluation for remediation of metal contaminated soil and water. J Environ Manag 92:2675–2682

Kamari A, Pulford ID, Hargreaves JSJ (2011b) Chitosan as a potential soil amendment to remediate metal contaminated soil – a characterisation study. Colloids Surf. B: Biointerf. 82:71–80

Kang K, Lee CG, Choi JW, Kim YK, Park SJ (2016) Evaluation of the use of sea sand, crushed concrete, and bentonite to stabilize trace metals and to interrupt their release from contaminated marine sediments. Water Air Soil Pollut 227: 308-320

Krishna AK, Govil PK (2004) Heavy metal contamination of soil around Pali industrial area, Rajasthan, India. Environ Geol 47(1): 38-44

Kumararaja P, Manjaiah KM, Datta SC, Shabeer TPA (2014) Potential of bentonite clay for heavy metal immobilization in soil. Clay Res 33 (2): 83-96

Kumararaja P, Manjaiah KM (2015). Adsorptive removal of Ni and Cd by bentonite from aqueous system. Ecol Environ Conser 21: S265-S272

Kumararaja P, Manjaiah KM, Datta SC, Sarkar B (2017) Remediation of metal contaminated soil by aluminium pillared bentonite: synthesis, characterisation, equilibrium study and plant growth experiment. Appl Clay Sci 137: 115-122

Lewandowska K, Sionkowska A, Kaczmarek B, Furtos G (2014) Characterization of chitosan composites with various clays. Int J Bio Macromolecules 65:534–541

Lim JE, Sung JK, Sarkar B, Wang H, Hashimoto Y, Tsang DCW, Ok YS (2016) Impact of natural and calcined starfish (Asterina pectinifera) on the stabilization of Pb, Zn and As in contaminated agricultural soil. Environ Geochem Health 39(2):431-441

Li P, Lang M, Wang XX, Zhang, T.L (2016) Sorption and desorption of copper and cadmium in a contaminated soil affected by soil amendments. Clean Soil Air Water 44: 1547–1556

Liu Q, Yang B, Zhang L, Huan R (2015) Adsorptive removal of Cr (VI) from aqueous solutions by cross-linked chitosan/bentonite composite. Korean J Chem Eng 32 (7): 1314-1322

Luo J, Han G, Xie M, Cai Z, Wang X (2015) Quaternized chitosan/montmorillonite nanocomposite resin and its adsorption behaviour. Iran Polym J 24:531–539

Ma Y, Shi F, Wang Z, Wu M, Ma J, Gao C (2012) Preparation and characterization of PSf/clay nanocomposite membranes with PEG 400 as a pore forming additive. Desalination 286: 131-137

McBride MB (1994) Environmental Chemistry of Soils. Oxford University Press, New York, NY, USA.

Ming H, Naidu R, Sarkar B, Lamb DT, Liu Y, Megharaj M (2016) Competitive sorption of cadmium and zinc in contrasting soils. Geoderma 268: 60–68

Moussout H, Ahlafi H, Aazza M, Zegaoui O, El Akili C (2016) Adsorption studies of Cu(II) onto biopolymer chitosan and its nanocomposite 5%bentonite/chitosan. Water Sci Technol 73(9): 2199-210

Naidu R (2013) Recent advances in contaminated site remediation. Water Air Soil Pollut 224 (12): 1–11

Ngah WWS, Teong LC, Toh RH, Hanafiah MAKM (2013) Comparative study on adsorption and desorption of Cu (II) ions by three types of chitosan–zeolite composites. Chem Eng J 223: 231–238

Paluszkiewicz C, Stodolak E, Hasik M, Blazewicz M (2011) FTIR study of montmorillonite-chitosan nanocomposite materials. Spectrochim Acta Part A 79: 784-788

Pereira FAR, Sousa KS, Cavalkanti GRS, Fonseca MG, Antonio GS, Alves APM (2013) Chitosan-montmorillonite biocomposite as an adsorbent for copper (II) cations from aqueous solutions Int J Biol Macromolecules 61: 471–478

Pereira FS, Lanfredi S, Gonzalez ERP, Agostini DLS, Gomes HM, Medeiros RS (2017) Thermal and morphological study of chitosan metal complexes. J Therm Anal Calorim 129(1):291-301

Pestov A, Bratskaya S (2016) Chitosan and its derivatives as highly efficient polymer ligands. Molecules 21(3):330 365

Rafiei HR, Shirvani M, Ogunseitan OA (2016) Removal of lead from aqueous solutions by a poly(acrylic acid)/ bentonite nanocomposite. Appl Water Sci 6:331–338Rinklebe J, Shaheen SM (2015) Miscellaneous additives can enhance plant uptake and affect geochemical fractions of copper in a heavily polluted riparian grassland soil. Ecotox Environ Safety 119: 58–65

Rusmin R, Sarkar B, Biswas B, Churchman J, Liu Y, Naidu R (2016) Structural, electrokinetic and surface properties of activated palygorskite for environmental application. Appl Clay Sci 134: 95-102

Rusmin R, Sarkar B, Liu Y, McClure S, Naidu R (2015) Structural evolution of chitosan–palygorskite composites and removal of aqueous lead by composite beads. Appl Surf Sci 353: 363-375

Samia M (2016) Chitosan-G-poly(acrylamide)/diatomite superabsorbent composites: synthesis and investigation of swelling properties. J Mater Proce Environ 4(1): 21-25

Saravanan D, Gomathi T, Sudha PN (2011) Sorption studies on heavy metal removal using chitin/bentonite biocomposite. Int J Biol Macromolecules 53: 67-71

Sarkar S (2009) Preparation of nanocomposite polymer for slow release fertilizer. Ph.D. Thesis, Division of Soil Science and Agricultural Chemistry, Indian Agricultural Research Institute, New Delhi, India.

Sarkar B, Naidu R, Rahman MM, Megharaj M, Xi Y (2012) Organoclays reduce arsenic bioavailability and bioaccessibility in contaminated soils. J Soils Sedim 12: 704-712

Sastre J, Rauret G, Vedal M (2006) Effect of the cationic composition of sorption solution on the quantification of sorption–desorption parameters of heavy metals in soils. Environ Pollut 140: 322–339

Shaheen SM, Rinklebe J (2015) Impact of emerging and low-cost alternative amendments on the (im)mobilization and phytoavailability of Cd and Pb in a contaminated floodplain soil. Ecol Eng 74: 319–326

Shaheen SM, Rinklebe J, Selim MH (2015) Impact of various amendments on immobilization and phytoavailability of nickel and zinc in a contaminated floodplain soil. Int J Environ Sci Technol 12 (9): 2765-2776

Shaheen SM, Tsadilas CD, Rinklebe J (2013) A review of the distribution coefficients of trace elements in soils: Influence of sorption system, element characteristics, and soil colloidal properties. Adv in Colloid Inter Sci 201–202: 43–56

Shaheen SM, Tsadilas CD, Rinklebe J (2015) Immobilization of soil copper using organic and inorganic amendments. J Plant Nutr Soil Sci 178: 112–117

Sheikh HA, Shirvani M, Shariatmadari H (2013) Competitive sorption of nickel, cadmium, zinc and copper on palygorskite and sepiolite silicate clay minerals. Geoderma 192:249–253

Souza Braz A, Fernandes A, Ferreira J, Alleoni L (2013) Distribution coefficients of potentially toxic elements in soils from the eastern Amazon. Environ Sci Pollut Res 20:7231–7242

Srinivasarao CH, Gayatri SR, Venkateswarlu B, Jakkula VS, Wani SP, Kundu S, Sahrawat KL, Rajasekha Rao BK, Marimuthu S, Gopala Krishna G (2014) Heavy metals concentration in soils under rainfed agro-ecosystems and their relationship with soil properties and management practices. Int J Environ Sci Technol 11(7):1959–1972

Tsadilas C, Shaheen SM, Samaras V, Gizas D, Hu Z (2009) Influence of fly ash application on copper and zinc sorption by acidic soil amended with sewage sludge. Commun Soil Sci Plant Analy 40: 273-284

Tsai WC, Buscano SI, Kan CC, Futalan CF, Dalida MLP, Meng-Wei W (2016) Removal of copper, nickel, lead, and zinc using chitosan-coated montmorillonite beads in single- and multi-metal system. Desalination Water Treat 57: 9799–9812

Tsai WC, de Luna MDG, Arriesgado HLPB, Futalan CM, Colades JI, Wan MW (2016) Competitive fixed-bed adsorption of Pb(ii), Cu(ii), and Ni(ii) from aqueous solution using chitosan-coated bentonite. Int J Poly Sci http://dx.doi.org/10.1155/2016/1608939

Uchimiya M, Klasson KT, Wartelle LH, Lima IM (2011) Influence of soil properties on heavy metal sequestration by biochar amendment: 1. Copper sorption isotherms and the release of cations. Chemos 82:1431–1437

Usman ARA (2008) The relative adsorption selectivities of Pb, Cu, Zn, Cd and Ni by soils developed on shale in New Valley, Egypt. Geoderma 144: 334–343

Wang H, Tang H, Liu Z, Zhang X, Hao Z, Liu Z (2014) Removal of cobalt (II) ion from aqueous solution by chitosan-montmorillonite. J Environ Sci 26: 1879-1884

Xie Y, Wang A (2009) Study on superabsorbent composites XIX. Synthesis, characterization and performance of chitosan-g-poly (acrylic acid)/vermiculite superabsorbent composites. J Polym Res 16:143–150

Xiong X, Stagnitti F, Allinson G, Turoczy N, Li P, LeBlanc M, Cann M A, Doerr SH, Steenhuis TS, Parlange JY, de Rooij G, Ritsema C J, Dekker LW (2005) Effect of clay amendments on adsorption and desorption of copper in water repellent soils. Austr J Soil Res 43: 397-402.

Yadav M, Rhee KY (2012) Superabsorbent nanocomposite (alginate-g-PAMPS/MMT): synthesis, characterization and swelling behavior. Carbohydr Polym 90(1):165–173.

Ye M, Sun M, Kengara FO, Wang J, Ni N, Wang L, Song Y, Yang X, Li H, Hu F, Jiang X (2013) Evaluation of soil washing process with carboxymethyl-β-cyclodextrin and carboxymethyl chitosan for recovery of PAHs/heavy metals/fluorine from metallurgic plant site. J Environ Sci 26: 1661-1672

Yin Z, Cao J, Li Z, Qiu D (2015) Reducing the bioavailability of cadmium in contaminated soil by dithiocarbamate chitosan as a new remediation. Environ Sci Pollut Res Int 22 (13): 9668–9675

Zhang C, Zhu MY, Zeng GM, Yu ZG, Cui F, Yang ZZ, Shen LQ (2016) Active capping technology: a new environmental remediation of contaminated sediment. Environ Sci Pollut Res 23(5): 4370 - 4375

Zhang J, Wang Q, Wang A (2007) Synthesis and characterization of chitosan-g-poly(acrylic acid)/attapulgite superabsorbent composites. Carbohydrate Polym 68: 367-374

Supplementary Information for:

Chitosan-g-poly(acrylic acid)-bentonite composite: a potential immobilizing agent of heavy metals in soil

P. Kumararaja[a,b], K. M. Manjaiah[a], S.C. Datta[a], T.P. Ahammed Shabeer[c] and Binoy Sarkar[d,e]

[a]Division of Soil Science and Agricultural Chemistry, ICAR-Indian Agricultural Research Institute, New Delhi, India

[b]ICAR-Central Institute of Brackishwater Aquaculture, Chennai, Tamil Nadu, India

[c]ICAR-National Research Centre for Grapes, Pune, Maharashtra, India

[d]Department of Animal and Plant Sciences, The University of Sheffield, Sheffield, S10 2TN, UK

[e]Future Industries Institute, University of South Australia, Mawson Lakes, SA 5095, Australia

SI Table 1: Comparison of metal adsorption capacities of chitosan bentonite composites

Material	Metal	Adsorption capacity (mg g^{-1})	Reference
Chitosan-montmorillonite beads	Cu	100	Pereira et al. 2013
Cross-linked chitosan/Al_{13}-pillared montmorillonite	Cu	53.3	Duan et al. 2014
PMAA/ grafted chitosan-bentonite	Cd	83	Abdel Khalek et al. 2012
Chitosan/vermiculite bio composite	Cd	58.5	Chen et al. 2018
Chitosan-clay composite	Ni	32.4	Futalan et al. 2011
Chitosan immobilized bentonite	Ni	18.7	Tirtom et al. 2012
Chitosan-GLA	Zn	37.7	Kamari et al. 2011
Chitosan-AA-bentonite composite	Zn	73.0	Present study
	Cu	88.5	
	Ni	48.5	
	Cd	51.6	

References

Abdel KMA, Mahmoud GA, El-Kelesh NA (2012) Synthesis and characterization of poly-methacrylic acid grafted chitosan-bentonite composite and its application for heavy metals recovery. Chem Mater Res 2: 1–12

Chen L, Wu P, Chen M, Lai X, Ahmed Z, Zhu N, Dang Z, Bi Y, Liu T (2018) Preparation and characterization of the eco-friendly chitosan/vermiculite biocomposite with excellent removal capacity for cadmium and lead. Appl Clay Sci /doi.org/10.1016/j.clay.2017.12.050

Duan L, Hu N, Wang T, Wang H, Ling L, Sun Y, Xie X (2016) Removal of copper and lead from aqueous solution by adsorption onto cross-linked chitosan/montmorillonite nanocomposites in the presence of hydroxyl–aluminum oligomeric cations: equilibrium, kinetic, and thermodynamic studies. Chem Eng Comm 203(1): 28-36

Futalan CM, Kan CC, Dalida ML, Hsien KJ, Pascua C, Wan MW (2011) Comparative and competitive adsorption of copper, lead, and nickel using chitosan immobilized on bentonite. Carbohyd Polym 83: 528-536

Kamari A, Pulford ID, Hargreaves JSJ (2011a) Binding of heavy metal contaminants onto chitosans—an evaluation for remediation of metal contaminated soil and water. J Environ Manag 92:2675–2682

Pereira FAR, Sousa KS, Cavalkanti GRS, Fonseca MG, Antonio GS, Alves APM (2013) Chitosan-montmorillonite biocomposite as an adsorbent for copper (II) cations from aqueous solutions. Int J Biol Macromolecules 61: 471–478

Tirtom VN, Dinçer A, Becerik S, Aydemir T, Çelik A (2012) Comparative adsorption of Ni(II) and Cd(II) ions on epichlorohydrin crosslinked chitosan–clay composite beads in aqueous solution. Chem Eng J 197:379-386.